

On the Methods of Determining the Radio Emission Geometry in Pulsar Magnetospheres

J. Dyks¹

Laboratory for High Energy Astrophysics, NASA/GSFC, Greenbelt, MD 20771, USA

`jinx@milkyway.gsfc.nasa.gov`

B. Rudak

Nicolaus Copernicus Astronomical Center, 87-100 Toruń, Poland

`bronek@ncac.torun.pl`

and

Alice K. Harding

Laboratory for High Energy Astrophysics, NASA/GSFC, Greenbelt, MD 20771, USA

`harding@twinkie.gsfc.nasa.gov`

ABSTRACT

We present a modification of the relativistic phase shift method of determining the radio emission geometry from pulsar magnetospheres proposed by Gangadhara & Gupta (2001). Our modification provides a method of determining radio emission altitudes which does not depend on the viewing geometry and does not require polarization measurements. We suggest application of the method to the outer edges of averaged radio pulse profiles to identify magnetic field lines associated with the edges of the pulse and, thereby, to test the geometric method based on the measurement of the pulse width at the lowest intensity level. We show that another relativistic method proposed by Blaskiewicz et al. (1991) provides upper limits for emission altitudes associated with the outer edges of pulse profiles. A comparison of these limits with the altitudes determined with the geometric method may be used to probe the importance of rotational distortions of magnetic field and refraction effects in the pulsar magnetosphere. We provide a comprehensive discussion of the assumptions used in the relativistic methods.

Subject headings: pulsars: general

¹NAS-NRC Research Associate, on leave from Nicolaus Copernicus Astronomical Center, Toruń, Poland

1. Introduction

Since the discovery of pulsars (Hewish et al. 1968) the geometry of radio emission from pulsar magnetospheres was interpreted in terms of emission from purely dipolar magnetic fields (eg. Radhakrishnan & Cooke 1969; Cordes 1978; Lyne & Manchester 1988; Blaskiewicz et al. 1991; Rankin 1993; Gil & Kijak 1993). This assumption is justified by relatively high emission altitudes in comparison with R_{ns} inferred for the radio emission ($\sim 0.01R_{\text{lc}}$, where $R_{\text{lc}} = cP/2\pi$ is the light cylinder radius and P is the rotation period of a neutron star with radius R_{ns}). Most importantly, however, radio emission from the dipolar magnetic field hopefully can be described by a sufficiently small number of parameters and a limited number of observational parameters. The word “hopefully” reflects a second crucial assumption applied for the radio emission beam: that distinguishable features in pulse profiles (conal components, the outer edges of a profile) are associated with the beam structure (eg. of concentric hollow cones of enhanced radio emission) which in the reference frame corotating with the neutron star (CF) is symmetric with respect to the plane containing the dipole magnetic moment $\vec{\mu}$ and the rotation axis. Without this disputable assumption, the number of parameters required to determine the emission geometry increases considerably and one is left with a multi-parameter theory to be compared with data from which only a few parameters can be deduced. Hereafter, the axial symmetry (in CF) of the radio emission beam is assumed; the problem of its justification is presented in Section 4.1.

To further constrain the parameter space, these two assumptions (I – dipolar magnetic field; II – symmetry of radio beam) are often supplemented with two additional simplifications: III – it is assumed that in the CF the bulk of radio waves is emitted in the direction which is tangent to the local magnetic field at an emission point; IV – identifiable features in pulse profiles (eg. maxima of conal components) observed in a narrow frequency band are interpreted as radiation from a very narrow range of altitudes. The assumption No. III requires relatively large Lorentz factors γ of radio emitting electrons. Hereafter we assume that the broadening of the pulse features due to the radiation from the low energy electrons is negligible, although it may be significant in reality. Our assumption is fully justified in the case of the most popular radiation mechanism – the curvature radiation, because the electron Lorentz factors must exceed ~ 100 for the curvature spectrum to extend up to the observation frequency (~ 300 MHz). Curvature radiation from low energy electrons ($\gamma \sim 10$) cannot broaden the profile because it does not extend to 10^2 MHz. The model-dependent estimates of γ cover a large range between 50 and 10^4 (eg. Ruderman & Sutherland 1975; Machabeli et al. 2001; Melrose 2004). For the rather conservative estimate of $\gamma \sim 100$ the corresponding angular size of the single electron radiation beam is $\gamma^{-1} \sim 0.5^\circ$, which is an order of magnitude smaller than the typical width of the radio beam corresponding to the mean pulse profile.

With the assumptions I–IV, the radio emission geometry becomes completely determined by four parameters: α , β , r , and ρ . Their meaning is the following: α is an inclination of the magnetic dipole with respect to the rotation axis (ie. the angle between the magnetic moment $\vec{\mu}$ and the angular velocity $\vec{\Omega} = 2\pi P^{-1}\hat{z}$). β is an “impact angle”, ie. the minimum angle between an observer’s line of sight and $\vec{\mu}$. This parameter is often replaced by $\zeta = \alpha + \beta$ – the angle between the observer’s line of sight and the rotational axis. The next parameter, r , is the radial distance of the radio emission region measured from the center of the neutron star. Hereafter, we will often use its normalized value $r' = r/R_{lc}$. The last parameter, ρ , is the half opening angle of the radio emission cone/beam, ie. it is the angle between the direction of radio emission in CF and $\vec{\mu}$. These four parameters determine completely the emission geometry in the sense that any additional information about the emission region (eg. coordinates of emission point in the dipole frame, with z-axis along $\vec{\mu}$) can be easily derived from textbook equations for the dipole geometry and spherical trigonometry (eg. Radhakrishnan & Cooke 1969; Cordes 1978; Gil et al. 1984).

One desired additional piece of information is an answer to the question “which magnetic field lines does the observed emission come from?”. Following standard conventions, we identify magnetic field lines by θ_{fp} – the colatitude of foot points of the magnetic field lines at the neutron star surface. With the radio emission altitude r and the beam radius ρ determined, the value of θ_{fp} can be easily calculated. The parameter θ_{fp} is often expressed in terms of a fraction of the polar cap angle: $\theta'_{fp} = \theta_{fp}/\theta_{pc}$, where $\theta_{pc} = \arcsin((R_{ns}/R_{lc})^{1/2})$.

These four quantities are to be deduced from radio data. In most cases, however, a model-dependent analysis of the radio data at a given frequency provides us with only two quantities: β , and $W(f)$, where $W(f)$ is the apparent width of the radio pulse profile, usually defined by some simple criterion (eg. measured at some fraction f of maximum intensity; a wide variety of f is employed: $f = 0.0005$ (Kijak & Gil 2003), $f = 0.1$ (Blaskiewicz et al. 1991), $f = 0.5$ (Rankin 1993), $f = 1$ (Gangadhara & Gupta 2001)). The value of the inclination angle α could in principle be determined along with β from the “rotating vector” model of polarization position angle swings (Radhakrishnan & Cooke 1969). In practice, however, a fit of the model to the observed position angle curve is much less sensitive to α than to β (Rankin 1993). Only in exceptional cases can both of these parameters be derived (Lyne & Manchester 1988; Blaskiewicz et al. 1991; von Hoensbroech & Xilouris 1997). This led Rankin (1990) to a formulation of a method of determining α which assumes that the apparent width of the core component does not depend on the impact angle β and that in all pulsars the core component originates from the same, low altitude. The observed width of the core component becomes then a universal function of the pulsar rotation period P and the dipole inclination α , allowing, thus, to determine the latter parameter.

We are provided, therefore, with just three parameters (α , β , W) instead of four. This limitation prompted the development of two kinds of methods to determine the geometry of the radio emitting region: 1) A purely geometric method which assumes that the lowest detectable emission at the leading and at the trailing edge of a radio pulse originates at the last open magnetic field lines, with $\theta_{\text{fp}} = \theta_{\text{pc}}$. With the fourth parameter assumed *a priori*, the method makes it possible to determine the radial position of radio emission r from the observed pulse width W_0 (eg. Cordes 1978; Gil & Kijak 1993; Kijak & Gil 1997; 1998; 2003; Kijak 2001; hereafter we will use the index ‘0’ to refer to the pulse with $W(f)$ at the lowest intensity level, ie. practically at $f = 0.0005 - 0.1$). The derived altitudes are a few tens of R_{ns} at observation frequency $\nu \sim 1$ GHz. 2) Methods of the second kind are able to derive the fourth observational parameter by a measurement of phase shifts of some profile features with respect to some fiducial points. The methods are relativistic in the sense that the phase shifts are caused by combined effects of aberration and propagation time delays due to the finite speed of light c (for brevity, the latter effect will hereafter be called retardation). The second methods are superior to the geometric method in that they do not assume *a priori* the value of the fourth parameter. However, they must rely on additional assumptions about the radio pulse profile. Gangadhara & Gupta (2001, hereafter GG2001) measure the relativistic phase shift of conal components with respect to the core component, which is assumed to originate from much lower altitude than the cones which surround it. Blaskiewicz et al. (1991, hereafter BCW91) measure the shift of pulse edges with respect to the center (or the “inflection point”) of the position angle curve which is assumed to originate from the same altitude as the emission at the outer wings of the profile. On average, the method of Blaskiewicz et al. (1991) (hereafter BCW method) gives emission radii in rough agreement with that of the geometric method (Gil & Kijak 1993; Kijak & Gil 1997; 1998; 2003). However, the method of GG2001 predicts notably larger values of r (by about factor of 2) than the geometric method. Unlike the geometric method (Cordes 1978; Gil & Kijak 1993), both relativistic methods (of GG2001 as well as BCW91) *in principle* make it possible to identify the radio emitting field lines. GG2001 and Gupta & Gangadhara (2003, hereafter GG2003) find θ'_{fp} in the range $0.22 - 0.74$ for radio emission observed at maxima of conal components. Unfortunately, the method of GG2001 can be applied only for pulsars having unambiguously identifiable pairs of conal components (and which possess a core component). So far, this has required application of a window thresholding technique (hereafter WT technique, GG2001) and limited application of the method only to a handful of the brightest objects. On the other hand, the BCW method suffers from a difficulty in finding the center of the position angle curve, and, as we show below, it yields values of θ'_{fp} exceeding 1. For convenience, hereafter we refer to the relativistic methods of GG2001 and BCW91 with the term “relativistic phase shift methods” (RPS methods).

In Section 2 we revise the method of GG2001, which results in a new formula for radio emission altitudes and furnishes the method with new interesting features. As noted in GG2003, the original method of GG2001 yielded radio emission altitudes larger than those derived with the geometric method. Our revision removes part of this discrepancy. In Section 3 we propose to apply the method to the outer edges of averaged pulse profiles. This will hopefully provide a test of the main assumption of the geometric method about the value of $\theta'_{\text{fp}} = 1$ for the beam edge. As an example, we try to perform such a test using the method of BCW91. In Section 4 we discuss in detail the assumptions of the relativistic methods. Our conclusions are in Section 5.

2. The modified relativistic phase shift method

The RPS method of Gangadhara & Gupta (2001) applies to pulsars with both core and cone emission, ie. for M and T pulsars in the classification scheme of Rankin (1983). Questionability of the conal pattern of radio emission beam will be discussed in Section 4.1. The model assumes that in the reference frame corotating with the neutron star the cones are symmetric around the narrow core beam. Obviously, in the case of the dipolar magnetosphere the second assumption can be most naturally accounted for by a model of the radio beam consisting of a narrow core beam centered at the dipole axis and a few nested hollow cones of enhanced radio emission surrounding the core. Magnetic field lines corresponding to a given cone have the same θ_{fp} and the same half-opening angle ρ at a fixed altitude. In fact, the second assumption can be made less stringent: it is sufficient for the conal beams to be symmetric with respect to the plane containing the core component and the rotation axis. Thus, the “conal” beams may have eg. elliptical crosssection with the core beam located in the plane containing the ellipse center and the rotation axis (ie. not necessary at the ellipse center). The possibility of the elliptical beam is discussed eg. in Mitra & Deshpande (1999).

The method starts with identifying the core component in the radio pulse profile. Then one attempts to identify the same number of conal components on both the leading and the trailing side of the core component. The innermost pair of two conal components located on both sides of the core is identified as emission from the same, innermost hollow cone of the radio beam. The next pair of conal components which bracket/flank the innermost pair is interpreted as emission from the next-to-innermost hollow cone of the radio beam, and so on. For each conal pair the observed phase of the leading component (ϕ_l) and the phase of the trailing component (ϕ_t) is measured with respect to the core component which defines the phase $\phi = 0$. As emphasized by GG2003 in all cases with clear identification of cones,

the conal components were shifted toward earlier phases with respect to the core component, ie. $|\phi_1| > \phi_t$. This effect was noticed already by Gil (1985), who proposed the retardation effect to explain the asymmetry. More correctly, GG2001 interpreted the asymmetry as a forward shift of conal components due to combined effects of aberration of conal emission and retardation of core emission. The (negative) relativistic phase shift $\Delta\phi_{\text{obs}}$ between the midway point of conal pairs and the core component is equal to:

$$\Delta\phi_{\text{obs}} = \frac{\phi_t - |\phi_1|}{2} \quad (1)$$

and the separation between the maxima of conal components is given by

$$W = \phi_t + |\phi_1| \quad (2)$$

The observed positions of the two conal components (ϕ_1 and ϕ_t) measured with respect to the core component are the *two* most desired observational parameters which replace the single W parameter. Beyond question, recognizing this point is a great insight of Gangadhara & Gupta (2001).

The next step in the method of GG2001 was to express $\Delta\phi_{\text{obs}}$ in terms of radial distance of conal radio emission r_{em} . In the absence of the aberration and retardation effects (hereafter AR effects), the center (ie. the maximum) of the core component as well as the center of the conal pair would be observed at the same fiducial phase ϕ_f which formally corresponds to emission from $r = 0$. In general, the radial distance r_{em} of the conal emission is different from the radial distance r_{cr} of the core emission. Therefore, the AR effects shift the center of the conal pair by $\Delta\phi(r_{\text{em}})$ with respect to ϕ_f , whereas the center of the core component is shifted with respect to ϕ_f by a different amount of $\Delta\phi(r_{\text{cr}})$. The observed shift is the difference between these: $\Delta\phi_{\text{obs}} = \Delta\phi(r_{\text{em}}) - \Delta\phi(r_{\text{cr}})$.

The value of $\Delta\phi$ is a sum of a shift due to the aberration and a shift due to the retardation: $\Delta\phi = \Delta\phi_{\text{ab}}(r) + \Delta\phi_{\text{ret}}(r)$, where the radial distance of radio emission r may refer either to r_{em} or r_{cr} . The retardation shift is equal to

$$\Delta\phi_{\text{ret}} \simeq -\frac{r}{R_{\text{lc}}}, \quad (3)$$

regardless of α and β , at least as long as the lowest order ($\sim r'$) relativistic effects are considered.

To first order in r/R_{lc} (cf. Appendix A; GG2001), the aberration changes the direction of photon emission by an angle:

$$\eta_{\text{ab}} \simeq \frac{v_{\text{rot}}}{c} \simeq \frac{r}{R_{\text{lc}}} \sin \zeta \quad (4)$$

where $\vec{v}_{\text{rot}} = \vec{\Omega} \times \vec{r}$ is the local corotation velocity at the emission point. Following the already published work (Cordes 1978; Phillips 1992), GG2001 assumed that the resulting phase shift $\Delta\phi_{\text{ab}}$ is equal to $-\eta_{\text{ab}}$. This is, however, not true in general, because the aberrated emission direction, when rotated by 360° around $\vec{\Omega}$, does not delineate a great circle on a sphere centered at the star. For this reason, the aberrational shift should be written in the form:

$$\Delta\phi_{\text{ab}} \simeq -\frac{\eta_{\text{ab}}}{\sin \zeta} \simeq -\frac{r}{R_{\text{lc}}}. \quad (5)$$

Eq. (5) reflects the fact that any decrease in the aberration angle η_{ab} caused by the smaller corotation velocity near the rotation axis is cancelled out by the small circle effect (eq. A8). A rigorous derivation of this approximate result can be found in Appendix A. Thus, the total relativistic shift with respect to ϕ_{f} is equal to $\Delta\phi \simeq -2r'$, whereas the observed shift of the conal pair with respect to the core is equal to $\Delta\phi_{\text{obs}} = -2(r_{\text{em}} - r_{\text{cr}})R_{\text{lc}}^{-1}$. The resulting formula for the altitude of the conal emission reads

$$h_{\text{em}} = r_{\text{em}} - r_{\text{cr}} \simeq -\frac{\Delta\phi_{\text{obs}}}{2}R_{\text{lc}}. \quad (6)$$

In the case $r_{\text{cr}} \ll r_{\text{em}}$, considered by GG2001:

$$r_{\text{em}} \simeq -\frac{\Delta\phi_{\text{obs}}}{2}R_{\text{lc}}. \quad (7)$$

This formula gives emission radii smaller by a factor $a \simeq (1 + \sin \zeta)/2$ than those obtained by GG2001 (cf. their eq. 9). As shown in Appendix A, the approximation (7) holds with accuracy of $\sim 10\%$ for $r' \lesssim 0.01$. For objects with moderate or large dipole inclinations ($\alpha \simeq 40^\circ - 90^\circ$) this is a minor correction, however, for nearly aligned rotators the radii become almost two times smaller. The method of GG2001 applies to broad pulse profiles with well resolved conal components. This criterion favours objects with small α , and, therefore, makes the modification important. GG2003 find particularly large emission radii for two objects, one of which (B2111+46) has very small inclination angle $\alpha = 9^\circ$. For this object, viewed at the angle $\zeta = 11.4^\circ$, our modification results in emission radii which are smaller by a factor of 0.6 than those derived by GG2003. For the second problematic pulsar (B2045–16), viewed at a considerably larger angle $\zeta = 37.1^\circ$, our modification does not reduce the radii significantly. GG2003 report some difficulties with unambiguous identification of conal pairs for this pulsar.

Using the values of ϕ_1 and ϕ_t published by GG2001 and GG2003 we recalculated the radio emission altitudes for objects studied therein. The resulting values are given in Table 1 (columns 5 and 6). The errors of h_{em} ($\sim 22\%$) are much larger than the errors of ϕ_1 and ϕ_t ($\sim 3\%$ as measured by Gangadhara & Gupta), because $h_{\text{em}} \propto \Delta\phi_{\text{obs}}$ and $\Delta\phi_{\text{obs}}$ is a very small difference between ϕ_t and $|\phi_1|$ (eq. 1).

We emphasize that our modification is not barely a rescaling of the method of GG2001, but it furnishes their method with completely new features. Unlike the original equation (9) of GG2001, our formula for the emission radius (eq. 7) *does not* depend on α and β , which is a valuable feature given the problems with determining α . A method of BCW91 is also independent of α and β , however, it requires high-quality polarization measurements, and can only be applied to pulsars with well ordered position angle swings. Our modification of the method of GG2001 provides a method for determining r , which not only can do without the knowledge of α and β , but at the same time it does not require the polarization measurements. It is based solely on information contained in M, and T-type profiles. The applicability of different methods to different sets of available data is summarized in Table 2. Since the presence of a core in pulse profiles is often accompanied by a disordered shape of the position angle curve (eg. Rankin 1993), the two methods (ie. the delay-radius relation of BCW91 and our eq. 7) can complement each other. On the other hand, this is a disadvantage, because it makes it difficult to compare the methods.

To identify magnetic field lines from which the conal emission originates, it is necessary to determine the half opening angle ρ of the emission cones. This is accomplished with the help of the cosine formula of spherical trigonometry, which connects the values of ρ , α , and ζ with the observed separation of conal components $W(f = 1)$:

$$\cos \rho = \cos \left(\frac{W}{2} \right) \sin \alpha \sin \zeta + \cos \alpha \cos \zeta. \quad (8)$$

This time the knowledge of α and ζ is necessary. Since the formula for ρ does not depend on r the values of ρ calculated by GG2001 and GG2003 are correct.

With ρ and r determined from eqs. (8) and (7), one can calculate the colatitude of footprints of active magnetic field lines at the star surface with the dipolar formula:

$$\theta_{\text{fp}} = \arcsin \left[\left(\frac{R_{\text{ns}}}{r} \left(\frac{2}{3} - \frac{1}{6} \left(x + (x^2 + 8x)^{1/2} \right) \right) \right)^{1/2} \right], \quad (9)$$

where $x = \cos^2 \rho$ (see Appendix A). In the small angle approximation ($\rho \ll 1$) the formula reduces to the well known approximate form:

$$\theta_{\text{fp}} \simeq \frac{2}{3} \rho \left(\frac{R_{\text{ns}}}{r} \right)^{1/2}. \quad (10)$$

Obviously, since the revised method predicts lower emission radii than its original version but the same opening angles ρ , it must yield larger footprint colatitudes θ_{fp} . Since, $\theta_{\text{fp}} \propto r^{-1/2}$ the values of θ_{fp} increase only by a factor of $b = (2/(1+\sin \zeta))^{1/2}$ between 1 and 1.4. Consequently,

the modified values of $\theta'_{\text{fp}} = \theta_{\text{fp}}/\theta_{\text{pc}}$ for objects studied by GG2001 and GG2003 are given in the last column of Table 1. They range from 0.28 to 0.88. The values of θ'_{fp} for the outermost cones cover the range between 0.35 and 0.88. The errors of θ'_{fp} are based only on the errors of ϕ_1 and ϕ_t determined by GG2001 and do not include the large uncertainties of α , and β .

Since our revision rescales the values of r and of θ_{fp} by factors which are the same for a given pulsar, the main findings of GG2001 and GG2003 (ie. higher altitudes for broader cones and lower altitudes for higher radio frequencies) remain valid.

3. Comparison of the RPS methods with the geometric method

In addition to the conal components, there is one more feature in radio pulse profiles which for a long time has been believed to be symmetric with respect to the $(\vec{\Omega}, \vec{\mu})$ plane – the outer edge of the radio beam. The assumption about the symmetry has always been present in the traditional, geometric method of determining radio emission altitudes (eg. Kijak & Gil 1997). Therefore, the method of GG2001 may also be applied to the edges of radio beam, not only to maxima of the conal components. Hereafter, the RPS method of GG2001 with this assumption will be referred to as the “outer edge relativistic phase shift method” (OERPS method). The method requires a measurement of ϕ_1 and ϕ_t for the outer edges of an *averaged* pulse profile. Then calculations of the original method of GG2001 can be performed (equations 1 – 9) to determine both the altitude and the locations θ'_{fp} of magnetic field lines for the radio emission at the pulse edge. Thus, the OERPS method may be used to test the geometric method which a priori assumes $\theta'_{\text{fp}}(\text{edge}) = 1$.

The OERPS method does not require an identification of conal components within the pulse profile. This method will work without the analysis of single pulses (with the WT technique) and it can be applied directly to averaged pulse profiles with large signal to noise ratio. A significant limitation of the OERPS method is that it requires very accurate measurements of the observed positions ϕ_1 and ϕ_t of the leading and the trailing edge of the radio pulse profile. These are much less defined than the positions of conal maxima. Therefore, the method may give less accurate results than the original RPS method of GG2001, unless very precise determination of ϕ_1 and ϕ_t is achieved. GG2001 and GG2003 found that shifts of outermost cones’ maxima with respect to the core may in some cases be as large as 3° , and they were able to measure some shifts with accuracy of $\sim 0.05^\circ$ ie. a few percent. A much larger error (typically $\sim 30\%$) is inherent in the OERPS method and in the method of BCW91 which must deal with locating the “lowest intensity” points.

Because we have no access to high-quality radio data to apply the OERPS method,

instead, below we try to use the BCW method to identify the active magnetic field lines. Like the OERPS method, the method of BCW91 provides the value of r in a way which is independent of α , β , and, most importantly, of θ_{fp} . The lowest intensity width W_0 (usually measured by BCW91 at the level of $f = 0.02$ and used to determine the center of a profile), along with α , β , and r , provides all necessary information to calculate θ_{fp} with the help of equations (8) – (9), ie. in the same way as in GG2001.

However, since different components of a pulse profile may originate from different altitudes, the values of r derived with some methods may represent an average over several components. To calculate θ_{fp} for the pulse edge, it is necessary to know the radial distance r_{edge} , which refers to the outer edges of the pulse profile. Establishing the relation between the pulse-averaged emission radius r , and the “edge radius” r_{edge} is an important step in determining θ_{fp} for the outer edge of the pulse profile. Normally, calculating θ_{fp} for the pulse edge would require using the equations (8) – (9) with $r = r_{\text{edge}}$. An easier way is to use the equation (10) which implies that the ratio of θ_{fp} corresponding to r_{edge} determined with some method, to $\theta_{\text{fp,geo}}$ of the geometric method is:

$$\frac{\theta_{\text{fp}}}{\theta_{\text{fp,geo}}} \simeq \theta'_{\text{fp}} \simeq \left(\frac{r_{\text{geo}}}{r_{\text{edge}}} \right)^{1/2}, \quad (11)$$

because $\theta_{\text{fp,geo}} = \theta_{\text{pc}}$ by assumption, which we want to verify. In the above formula $\theta_{\text{fp,geo}}$ and r_{geo} refer to the geometric method, whereas θ_{fp} and r_{edge} refer to another method.¹ The above equation holds only when r_{edge} (and θ_{fp}) refer to the outer edge of a pulse profile, just as the values of r_{geo} do. Emission radii provided by the BCW method (hereafter denoted by r_{delay}) are calculated under the assumption that all components in a pulse profile originate from the same altitude, ie. $r_{\text{edge}} = r_{\text{delay}}$ by assumption. Thus, inserting $r_{\text{edge}} = r_{\text{delay}}$ into eq. (11) one can calculate θ'_{fp} predicted by the BCW method for the pulse edge.

We use the values of r_{delay} and r_{geo} calculated for the same data set by BCW91 and presented in their table 3. The values of θ'_{fp} derived with the BCW method for seven clean-cut cases with reasonably small statistical errors, and most probably free from systematic errors, are presented in column 3 of Table 2. Column 4 presents a range of θ'_{fp} allowed by 1σ errors derived for r_{delay} and r_{geo} by BCW91 (table 3 therein). The last column shows the level of consistency of the two methods (in σ), ie. the level at which the derived values are consistent with $\theta'_{\text{fp}} = 1$.

According to Table 2, for four cases (B0301+19 and B0525+21, both at 0.43 and 1.4 GHz) the BCW method yields $\theta'_{\text{fp}} > 1$, ie. radio emission from the closed magnetic field line

¹For brevity, in eq. (11) we skip the index ‘edge’ at θ_{fp} and θ'_{fp} , which hereafter should be understood as referring to the outer edge of the pulse profile.

region. The inconsistency with $\theta'_{\text{fp}} = 1$ is at $\sim 2\sigma$ level. The result $\theta'_{\text{fp}} > 1$ is equivalent to $r_{\text{edge}} < r_{\text{geo}}$ (cf. eq. 11), and, therefore may result from underestimating r_{edge} and/or from overestimating r_{geo} . As noted by BCW91, contrary to the assumption $r_{\text{edge}} = r_{\text{delay}}$, the values of r_{edge} may actually be larger than r_{delay} , because r_{delay} represents an average over the pulse profile, and inner parts of the profile may originate from lower altitudes than the outer edges of the pulse (eg. Rankin 1993; GG2001). Below we show, however, that even if the central parts of the pulse profiles originated from the star surface, the values of r_{edge} cannot exceed $2r_{\text{delay}}$. In the BCW method, the values of r_{delay} are derived from the relative position of the outer edges of the profile and the center of the position angle (PA) curve. Let us assume that the center of the PA curve is determined mostly by the central parts of profiles which may originate from lower altitudes than the beam edge. Let us define a fiducial phase zero as a moment at which an observer detects a light signal emitted from the neutron star center when the dipole axis was located in the plane containing the rotation axis and the observer's position. The star's rotation shifts the profile center (determined by the midpoint between the *outer edges* of the pulse) toward earlier phases by $-2r_{\text{edge}}/R_{\text{lc}}$ with respect to the fiducial phase, where r_{edge} is the radial distance for emission at the edge of the pulse profile. At the same time, the rotation delays the center of the position angle swing by $2r_{\text{in}}/R_{\text{lc}}$ with respect to the fiducial phase, where r_{in} refers to the radiation from inner parts of the profile which determine the position of the center of the PA swing, according to our working hypothesis. For the case considered by BCW91 (ie. $r_{\text{edge}} = r_{\text{in}}$), the total shift is $4r_{\text{edge}}/R_{\text{lc}}$. For the other limiting case $r_{\text{edge}} \gg r_{\text{in}}$ the total shift is two times smaller: $2r_{\text{edge}}/R_{\text{lc}}$, since the delay of the center of the PA curve with respect to the fiducial phase is negligible. In this extreme case the value of r_{edge} derived from the shift $\Delta\phi_{\text{PA}}$ between the center of the PA curve and the profile center is given by:

$$r_{\text{edge}} = \frac{\Delta\phi_{\text{PA}}}{2} R_{\text{lc}} = 2r_{\text{delay}} \quad (\text{for } r_{\text{edge}} \gg r_{\text{in}}). \quad (12)$$

Therefore, in general the emission radii for the beam edge may be at most two times larger than r_{delay} derived by BCW91 for the case of $r_{\text{edge}} = r_{\text{in}}$:

$$r_{\text{edge}} \leq 2r_{\text{delay}}, \quad (13)$$

Using the upper limit of $r_{\text{edge}} = 2r_{\text{delay}}$ in eq. (11), would decrease the values of θ'_{fp} in Table 2 by a factor of $2^{-1/2}$. In spite of the large error range for θ'_{fp} (column 4 in Table 2), this would make only *two* of the four problematic values consistent with 1 within the level of 1σ . The other two values of θ'_{fp} (for B0301+19 at 1.42 GHz and B0525+21 at 0.43 GHz) would still remain inconsistent with 1 at 1σ level. Thus, lower emission altitudes for the central parts of profiles are not able to remove the disagreement completely. Indeed, different locations of emission regions for the conal peaks and for the bridge between them have been proposed for

the two pulsars based on different spectra and fluctuation properties (Backer 1973; Rankin 1983; BCW91). For B0525+21, BCW91 suggest the contribution of a quadrupole component of stellar magnetic field as a source of the error in r_{delay} . The underestimate of r_{delay} may also be caused by the rotationally-induced magnetic field line sweep-back, since the effect produces a shift of opposite sign to the shift $\Delta\phi_{\text{PA}}$ found by BCW91. The significance of this effect will be investigated in a forthcoming paper.

The result $\theta'_{\text{fp}} > 1$ (or $r_{\text{edge}} < r_{\text{geo}}$) could also arise due to an overestimate of r_{geo} . This may be caused by refraction effects, which would broaden the radio beam with altitude (Lyubarskii & Petrova 1998). However, this effect could be compensated (or even dominated) by the unavoidable underestimate of r_{geo} which is inherent to the method of its derivation: the geometric method associates the maximum value of $\theta'_{\text{fp}} = 1$ with the observed pulse width, whereas the true value of θ'_{fp} may well be smaller due to an inactivity of the outer parts of the polar cap and/or due to a limited sensitivity threshold. Therefore, in the case of the rectilinear propagation of radio waves, the values of r_{geo} should be considered as lower limits for r_{edge} . In consequence, it is worth noting that BCW91 underestimated their geometric radii r_{geo} , because these were calculated for the 10% intensity level ($f = 0.1$) instead of the lowest intensity level, which BCW91 usually identified with 2% of maximum intensity. Therefore, the values of θ'_{fp} in Table 2 are underestimated, and the actual disagreement of the BCW method with the condition $\theta'_{\text{fp}} \leq 1$ is even larger than given in the last column of Table 2.

For B1914+13 an upper limit for θ'_{fp} equal to 0.8 is given in Table 2 (based on r_{geo} and r_{delay} from table 3 of BCW91). This is the only case (of single core type – S_t), for which $\theta'_{\text{fp}} < 1$. Obviously, this could equally well imply the inactivity of the outer part of the polar cap as our inability to detect the outer wings of radio profiles. In either case, the assumption that $\theta'_{\text{fp}} = 1$ at the *observed* profile edge would be invalidated. We emphasize, that like any value of θ'_{fp} in Table 2, the upper limit of $\theta'_{\text{fp}} = 0.8$ may be underestimated because of the relatively high level of intensity (10%) for which the values of r_{geo} were calculated in BCW91.

Thus, by selecting a sample of pulsars studied by BCW91 with the smallest statistical errors, and least probable to be affected by systematic errors, we find that the BCW method implies the radio emission from the region of closed magnetic field lines, (ie. with $\theta'_{\text{fp}} > 1$), at the level $> 2\sigma$ in some cases. The way out would be to postulate either significant magnetic field deviations from the static dipole shape, or refraction effects (Lyubarskii & Petrova 1998). The distortions of the magnetic field may be caused by the presence of the quadrupolar stellar magnetic field (BCW91), or due to the rotationally induced sweep-back (Shitov 1983).

4. Discussion of assumptions of the relativistic phase shift methods

4.1. Asymmetry of the radio beam

To provide reliable estimates of r the RPS method of GG2001 requires the symmetry of cones of enhanced radio emission with respect to the plane containing the core component and the rotation axis. To calculate θ_{fp} , the core/cones system must be centered at the dipole axis. The OERPS method requires the same symmetry for the outer edge of the radio beam, and the BCW method requires the symmetry of the beam edge with respect to the $(\vec{\Omega}, \vec{\mu})$ plane, regardless of the position of the core component. All these assumptions are related to the old problem: is the beam shape conal or patchy? The patchy beam would invalidate all these methods. Fortunately, however, statistical analyses of distribution of components within the radio pulse provide arguments for the conal shape (eg. Mitra & Deshpande 1999; Kijak & Gil 2002; Gil et al. 2002). It seems that arguments for patchy structure of the beam (Lyne & Manchester 1988, hereafter LM88) are not equally strong. In addition to the effects described by Gil et al. (1993), the aberration and the retardation may enhance the *apparent* patchiness of the beam. This is because central components of pulse profiles seem to originate from lower altitudes than the outer components (eg. Rankin 1993; GG2001). The aberration and retardation effects shift the relative positions of different components in phase by $\Delta\phi \simeq 2\Delta r'$, where $\Delta r'$ is the difference of emission radii between different components in units of R_{lc} . Estimating $\Delta r' \sim 0.01$ one obtains $\Delta\phi \sim 1^\circ$ which amounts to $\sim 13\%$ of pulse width observed for pulsars with large dipole inclinations ($\alpha \sim 90^\circ$). Given that observed separation between components is much smaller than the pulse width (say 20 – 40%), these shifts, different for different objects because of diversity of r , along with other factors (eg. inexactly determined impact angles β) could easily produce the apparently random distribution of components within the pulse window, ie. in figures like the fig. 12 in LM88.

Other arguments for the conal beam shape are provided directly by the WT technique of GG2001. For 6 (out of 7) objects studied by GG2001 and GG2003, the same number of conal components was found on both sides of the core component, and only B2045–16 is a *possible* exception. In all cases, strong (ie. easily identifiable) components on the leading side corresponded to strong components on the trailing side, whereas new weak components, detected with the WT technique on one side of the core were always associated with weak components on the other side. It is natural to interpret this coincidence in terms of the conal, not patchy beam shape. Another interesting implication of this relation is the possibility of applying the method of GG2001 to a larger number of T and M pulsars, without the necessity of identification of all cones with the WT technique.

Thus, the conal beam shape seems to be consistent with observations. On theoretical grounds, the conal shape is supported by a model of sparks rotating around the magnetic pole due to the $\vec{E} \times \vec{B}$ drift (Ruderman & Sutherland 1975; Gil & Sendyk 2000). The model, as well as the conal beam hypothesis, is supported by observations of subpulse drifts (Gil & Krawczyk 1997; Deshpande & Rankin 1999; Vivekanand & Joshi 1999).

4.2. The reference altitude

All three RPS methods rely on a measurement of a shift between three identifiable points within a pulse profile and make assumptions about relative altitudes of these points. The method of GG2001 provides the *altitude* of the conal radio emission measured with respect to the altitude of the core emission (eq. 6). To identify the active magnetic field lines (ie. to calculate θ'_{fp}) it is necessary either to know r_{cr} or to rely on the assumption $r_{\text{cr}} \ll r_{\text{em}}$ (as we did in Table 1) which effectively means that the derived values of θ'_{fp} are upper limits.

There is a very simple geometric argument against the hypothesis that the core components originate from the very vicinity of the star surface: With the only exception of B1237+25, for all other objects studied by GG2001 and GG2003, and listed in our Table 1, the impact angles β are *larger* than the half opening angle of the last open field lines at the surface of the neutron star with radius $R_{\text{ns}} = 10$ km. Had the central components (identified as cores) originated close to the surface, our line of sight should miss them. Therefore, the impact angles determined for these objects from fitting the position angle swing are in clear disagreement with the assumptions of the method of determining α proposed by Rankin (1990). Assuming rectilinear propagation of radio waves, this discrepancy can be interpreted only in two ways: 1) either the radial distance for the core emission is much larger than R_{ns} , or 2) the impact angles β are systematically overestimated. In the first case, the dipole inclination angles α derived with Rankin’s method would be underestimated, at least as long as the width of the core beam is assumed to reflect the width of the open field line region at a given altitude. For the time being, it seems to be a matter of personal preference which of the possibilities (either 1. or 2.) is the case – Rankin (1990) assumed that the values of β are in error. Regardless of the choice, however, either α (based on the assumption $r_{\text{cr}} \sim R_{\text{ns}}$) or β *must* be in error, since they contradict each other. Therefore, the values of θ'_{fp} given in the last column of our Table 1 should be treated with caution.

PSR B0450–18, studied by GG2003 has the largest impact angle ($\beta \simeq 4^\circ$) among all the objects listed in Table 1. The half opening angle of the open field line region at the surface of the pulsar is equal to $1.5\theta_{\text{pc}} \simeq 1.68^\circ$. To exhibit the estimated width of $\sim 8^\circ$ (Rankin 1993), the central component in the pulse profile of this object would have to originate from

radial distance $r_{\text{cr}} \simeq 67$ km, assuming the uncertain values of $\alpha = 24^\circ$, $\beta = 4^\circ$ and $\theta'_{\text{fp}} = 1$ from Rankin (1990). This value is larger than the error of h_{em} estimated for this object in Table 1 and should be added to h_{em} to obtain r_{em} . Had the core component not filled in the open field line region, the value of r_{cr} would be even larger.

The RPS method of BCW91 assumes that radio emission at the edge of a profile originates from *the same* altitudes as the emission which determines the center of the position angle curve, in which case the predicted shift is equal to $4r_{\text{delay}}/R_{\text{lc}}$. As noted above this assumption, if not satisfied, would lead to an underestimate of emission altitudes for the outer edge of a profile. As shown in Section 3, however, the values of r_{edge} cannot exceed $2r_{\text{delay}}$.

5. Conclusions

We have modified the relativistic method of GG2001 of determining the radio emission geometry within pulsar magnetospheres. Our modification results in a method of determining the radio emission altitudes which does not depend on viewing geometry nor does it require polarization measurements. According to this method, the altitude of the radio emission region in units of R_{lc} is equal to a half of the relativistic phase shift of a pair of conal components with respect to the core component. We propose to extend application of the revised method to the outer edge of radio pulse profiles to identify magnetic field lines associated with the edge. This may provide a test of the geometric method of determining r , based on a measurement of a pulse width at the lowest intensity level.

As noted by GG2003, the radio emission radii derived with their original method for the outermost cones were notoriously larger than the radii derived for the pulse edge with the geometric method by Kijak & Gil (1997; 1998). Our revision has removed part of this discrepancy. However, since the geometric method assumes that the observed radio emission fills in the open field line region entirely ($\theta'_{\text{fp}} = 1$), the emission radii derived with the geometric method should be considered as lower limits for r_{edge} (provided the refraction effects can be neglected). Therefore, other methods of determining r_{edge} for the pulse edge should always yield $r_{\text{edge}} \geq r_{\text{geo}}$.

We determined the values of θ'_{fp} for the pulse edge at the 10% level using the relativistic method of Blaskiewicz et al. (1991). This has revealed that in individual cases the method often implies emission from the region of closed magnetic field lines. BCW91 associated this with the fact that the emission radii r_{delay} determined with their method may be smaller than r_{edge} because inner parts of pulse profiles can originate from lower altitudes. We have

shown that even accounting for this, the value of r_{edge} cannot exceed $2r_{\text{delay}}$, which is still not sufficient to solve the problem. Apparently, other effects, like the rotation-induced sweep-back of the magnetic field lines, or refraction effects may be responsible for the discrepancy.

JD thanks V. S. Beskin for comments on pulsar magnetosphere. We are grateful to J. Gil and R. Gangadhara for their valuable comments on the manuscript. We appreciate the comments of the anonymous referee who helped us to improve the paper significantly. This work was performed while JD held a National Research Council Research Associateship Award at NASA/GSFC. The work was also supported by the grant 2P03D.004.24 (JD and BR).

A. Derivation of equations (4), (5), and (9).

Let the radio waves in the reference frame corotating with the star be emitted in the direction \vec{k}' at angle ζ' with respect to the rotation axis. Because of the aberration, in the inertial observer frame the emission direction will be $\vec{k} \neq \vec{k}'$, and the observer will have to be located at an angle ζ with respect to $\vec{\Omega}$ to detect the radiation (see Fig. 1). In general, ζ differs from ζ' (eg. Kapoor & Shukre 1998). The unit vectors of the emission directions \vec{k}' and \vec{k} are related by the aberration formula:

$$\vec{k} = \frac{\vec{k}' + [\gamma + (\gamma - 1)(\vec{\beta}_{\text{rot}} \cdot \vec{k}')/\beta_{\text{rot}}^2]\vec{\beta}_{\text{rot}}}{\gamma(1 + \vec{\beta}_{\text{rot}} \cdot \vec{k}')} \quad (\text{A1})$$

where $\vec{\beta}_{\text{rot}}$ is the local corotation velocity in units of the speed of light c , and $\gamma = (1 - \beta_{\text{rot}}^2)^{-1/2}$ (eg. Dyks & Rudak 2003). Neglecting the terms of the order of β_{rot}^2 and higher, the above formula reduces to:

$$\vec{k}(1 + \vec{\beta}_{\text{rot}} \cdot \vec{k}') \approx \vec{k}' + \vec{\beta}_{\text{rot}}. \quad (\text{A2})$$

Eq. (10) implies that in the small angle approximation (ie. for emission from within the open field line region at altitudes $r \ll R_{\text{lc}}$) the value of the term $\vec{\beta}_{\text{rot}} \cdot \vec{k}'$ is limited as follows

$$\vec{\beta}_{\text{rot}} \cdot \vec{k}' \leq \beta_{\text{rot}} \cos \left[\frac{\pi}{2} - \frac{3}{2}(r')^{1/2} \right] = \beta_{\text{rot}} \sin[1.5(r')^{1/2}] \sim (r')^{3/2}, \quad (\text{A3})$$

where $r' = r/R_{\text{lc}} \ll 1$ is the radial distance of emission. Neglecting this term, one obtains

$$\vec{k} \approx \vec{k}' + \vec{\beta}_{\text{rot}} \quad (\text{A4})$$

with accuracy of the order of $(r')^{1/2}$ (ie. with 10% error for radio emission at 1% of R_{lc} ; hereafter we will use $r' = 0.01$ in all estimations). Therefore, to the first order in r' , the

aberration angle η_{ab} between \vec{k} and \vec{k}' is approximately equal to β_{rot} . By applying the cosine theorem of spherical trigonometry to the spherical triangle ABC in Fig. 1:

$$\cos \zeta = \cos \zeta' \cos \beta_{\text{rot}} + \sin \zeta' \sin \beta_{\text{rot}} \cos \frac{\pi}{2} \quad (\text{A5})$$

and neglecting the β_{rot}^2 terms and higher, one finds that

$$\zeta \approx \zeta', \quad (\text{A6})$$

ie. the aberration does not change the colatitude of photon emission direction measured with respect to $\vec{\Omega}$ (to the order of β_{rot}).

Application of the sine theorem to the ABC triangle:

$$\frac{\sin \Delta\phi_{\text{ab}}}{\sin \eta_{\text{ab}}} = \frac{\sin(\pi/2)}{\sin \zeta} \quad (\text{A7})$$

gives, for $\Delta\phi_{\text{ab}} \ll 1$, and $\eta_{\text{ab}} \ll 1$, the relation:

$$\Delta\phi_{\text{ab}} \approx \frac{\eta_{\text{ab}}}{\sin \zeta}, \quad (\text{A8})$$

used in eq. (5) (the minus sign in eq. (5) has been inserted to account for the fact that larger azimuths correspond to earlier detection phases). Eq. (A4) implies that $\eta_{\text{ab}} \approx \beta_{\text{rot}}$, ie.:

$$\eta_{\text{ab}} \approx r' \sin \theta = r' \sin(\zeta + \delta), \quad (\text{A9})$$

where θ is the colatitude of the emission point (measured from the rotation axis) and $\delta = \theta - \zeta$ so that $|\delta| \approx 3^{-1}|\beta| \leq 2^{-1}(r')^{1/2} \ll 1$, with β being the impact angle. Thus, for $|\delta| \ll 1$ and $|\delta| \ll \zeta$, one obtains

$$\eta_{\text{ab}} \approx r' \sin \zeta \left(\cos \delta + \frac{\sin \delta}{\tan \zeta} \right) \approx r' \sin \zeta, \quad (\text{A10})$$

which proves eq. (4). The neglected term $\sin \delta / \tan \zeta$ becomes large for the nearly aligned geometry. In general, ie. allowing for the maximum possible range of impact angles β between $\pm 1.5(r')^{1/2}$, the resulting error in η_{ab} could be equal to 10% for ζ as large as 30° . In the context of the RPS models discussed in this paper, however, the angle ζ corresponding to the 10% error will be much smaller. This is because the line of sight must traverse nearly through the center of the open field line region for the core/cone structure to be discernible, ie. $\beta \sim \varepsilon 1.5(r')^{1/2}$ with the parameter ε considerably smaller than 1. Adopting a reasonable value for ε , eg. $\varepsilon \sim 0.2$, one finds that the error of η_{ab} exceeds 10% when $\zeta \leq 6^\circ$.

Inserting eq. (A10) into eq. (A8) gives $\Delta\phi_{\text{ab}} \approx r'$ and proves eq. (5) The independence of $\Delta\phi_{\text{ab}}$ on ζ results directly from the fact that the decrease in the aberrational angle η_{ab}

for the line of sight approaching the rotation axis (eq. A10) is cancelled out by the “small circle” effect (eq. A8). Thus, we find that *as long as the emission direction in the CF does not deviate much from the meridional plane, the aberrational phase shift does not depend on viewing geometry (ie. neither on α nor on ζ)*. The simplicity of the delay-radius relation derived in BCW91 has the same origin.

We now turn to the derivation of eq. (9). Let $\vec{\mu}$ be the magnetic moment of the dipole, and let \vec{k}' be the emission direction tangent to the local magnetic field in the CF. The equation of the dipolar magnetic field lines is: $r^{-1} \sin^2 \theta_m = \text{const}$, where θ_m is the colatitude of the emission point in the reference frame with \hat{z} axis along $\vec{\mu}$. This equation implies that

$$\theta_{\text{fp}} = \arcsin \left[\left(\frac{R_{\text{ns}}}{r} \sin^2 \theta_m \right)^{1/2} \right], \quad (\text{A11})$$

where R_{ns} is the radius of the neutron star. The angle $\rho = \angle(\vec{\mu}, \vec{k}')$ is given by

$$\cos \rho = \frac{\vec{\mu} \cdot \vec{k}'}{|\vec{\mu}|} = \frac{3 \cos^2 \theta_m - 1}{(1 + 3 \cos^2 \theta_m)^{1/2}} \quad (\text{A12})$$

By calculating θ_m from eq. (A12) and inserting into (A11) one obtains eq. (9). The uncertainty of R_{ns} , present in eq. (A11), does not affect the ratio $\theta_{\text{fp}}/\theta_{\text{pc}}$, as long as $\theta_{\text{fp}} \ll 1$. The measurement errors of ϕ_1 and ϕ_t result in the error of θ_{fp} mainly through the inverse square root dependence on r . The error of the cones’ separation W (which enters the formula (9) through eq. 8) is negligible. This is because $\Delta\phi_{\text{obs}}$ (and, thereby, r) is calculated as a *small difference* between ϕ_t and $|\phi_1|$ (with $\phi_t \simeq |\phi_1|$) whereas W is a sum of these (cf. eqs. 1 and 2 and the comments in Sec. 2). The dependence $\theta_{\text{fp}} \propto r^{-1/2}$ implies that the fractional error of θ_{fp} ($\sim 13\%$) is approximately two times smaller than the fractional error of r (cf. columns 5 and 7 in Table 1).

REFERENCES

- Backer, D. C. 1973, ApJ, 182, 245
- Blaskiewicz, M., Cordes, J. M., & Wasserman, I. 1991, ApJ, 370, 643 (BCW91)
- Cordes, J. M. 1978, ApJ, 222, 1006
- Deshpande, A. A., & Rankin, J. M. 1999, ApJ, 524, 1008
- Dyks, J., & Rudak, B. 2003, ApJ, 598, 1201

- Gangadhara, R. T., & Gupta, Y. 2001, *ApJ*, 555, 31 (GG2001)
- Gil, J. 1985, *ApJ*, 299, 154
- Gil, J., Gronkowski, P., & Rudnicki, W. 1984, *A&A*, 132, 312
- Gil, J. A., & Kijak, J. 1993, *A&A*, 273, 563
- Gil, J. A., Kijak, J., & Seiradakis, J. H. 1993, *A&A*, 272, 268
- Gil, J., & Krawczyk, A. 1997, *MNRAS*, 285, 561
- Gil, J. A., & Sendyk, M. 2000, *ApJ*, 541, 351
- Gil, J., Gupta, Y., Gothoskar, P. B., & Kijak, J. 2002, *ApJ*, 565, 500
- Gupta, Y., & Gangadhara, R. T. 2003, *ApJ*, 584, 418 (GG2003)
- Hewish, A., Bell, S. J., Pilkington, J. D. H., Scott, P. F., & Collins, R. A. 1968, *Nature*, 217, 709
- von Hoensbroech, A., & Xilouris, K. M. 1997, *A&A*, 324, 981
- Kapoor, R.C., & Shukre, C.S. 1998, *ApJ*, 501, 228
- Kijak, J. 2001, *MNRAS*, 323, 537
- Kijak, J., & Gil, J. 1997, *MNRAS*, 288, 631
- Kijak, J., & Gil, J. 1998, *MNRAS*, 299, 885
- Kijak, J., & Gil, J. 2002, *A&A*, 392, 189
- Kijak, J., & Gil, J. 2003, *A&A*, 397, 969
- Lyne, A. G., & Manchester, R. N. 1988, *MNRAS*, 234, 477 (LM88)
- Lyubarskii, Y. E., & Petrova, S. A. 1998, *A&A*, 333, 181
- Machabeli, G., Khechinashvili, D., Melikidze, G., & Shapakidze, D. 2001, *MNRAS*, 327, 984
- Melrose, D. 2004, *Young Neutron Stars and Their Environments*, IAU Symposium, Vol. 218, eds. F. Camilo, & B. M. Gaensler, in the press (astro-ph/0308471)
- Mitra, D., & Deshpande, A. A. 1999, *A&A*, 346, 906
- Phillips, J. A. 1992, *ApJ*, 385, 282

- Radhakrishnan, V., & Cooke, D. J. 1969, *Astrophys. Lett.*, 3, 225
- Rankin, J. M. 1983, *ApJ*, 274, 333
- Rankin, J. M. 1990, *ApJ*, 352, 247
- Rankin, J. M. 1993, *ApJ*, 405, 285
- Romani, R. W. & Yadigaroglu, I.-A., 1995, *ApJ*, 438, 314
- Ruderman, M. A., & Sutherland, P. G. 1975, *ApJ*, 196, 51
- Shitov, Y. P. 1983, *Soviet Astr.*, 27, 314
- Vivekanand, M., & Joshi, B. C. 1999, *ApJ*, 449, 211

Table 1. Altitudes h_{em} of conal radio emission and surface colatitudes θ'_{fp} of magnetic field lines associated with the cones derived with the relativistic phase shift method of GG2001 with the modification applied according to eq. (6) of Section 2. The numbers are based on cones' shifts measured by GG2001 and GG2003 and α and β values from Rankin (1993) (cf. table 1 in GG2001 and GG2002).

| Pulsar | P [s] | ν [MHz] | Cone ^a | h_{em} [km] | h_{em} [% of R_{lc}] | θ'_{fp} |
|----------|---------|-------------|-------------------|----------------------|---|-----------------------|
| B0329+54 | 0.7145 | 325 | 1 | 150 ± 080 | 0.44 | 0.58 ± 0.17 |
| | | 325 | 2 | 330 ± 060 | 0.96 | 0.57 ± 0.06 |
| | | 325 | 3 | 600 ± 080 | 1.74 | 0.57 ± 0.05 |
| | | 325 | 4 | 880 ± 240 | 2.57 | 0.65 ± 0.12 |
| | | 606 | 1 | 120 ± 070 | 0.35 | 0.65 ± 0.22 |
| | | 606 | 2 | 280 ± 050 | 0.83 | 0.58 ± 0.06 |
| | | 606 | 3 | 460 ± 140 | 1.35 | 0.61 ± 0.11 |
| | | 606 | 4 | 640 ± 180 | 1.88 | 0.71 ± 0.12 |
| B0450–18 | 0.5489 | 318 | 1 | 230 ± 25 | 0.88 | 0.65 ± 0.04 |
| B1237+25 | 1.3824 | 318 | 1 | 160 ± 40 | 0.24 | 0.34 ± 0.06 |
| | | 318 | 2 | 411 ± 30 | 0.62 | 0.43 ± 0.02 |
| | | 318 | 3 | 540 ± 20 | 0.81 | 0.62 ± 0.01 |
| B1821+05 | 0.7529 | 318 | 1 | 230 ± 100 | 0.64 | 0.49 ± 0.12 |
| | | 318 | 2 | 320 ± 090 | 0.89 | 0.65 ± 0.11 |
| | | 318 | 3 | 440 ± 080 | 1.23 | 0.72 ± 0.08 |
| B1857–26 | 0.6122 | 318 | 1 | 160 ± 50 | 0.55 | 0.72 ± 0.12 |
| | | 318 | 2 | 350 ± 30 | 1.20 | 0.81 ± 0.04 |
| | | 318 | 3 | 480 ± 80 | 1.65 | 0.88 ± 0.08 |
| B2045–16 | 1.9617 | 328 | 1 | 1000 ± 130 | 1.06 | 0.31 ± 0.030 |
| | | 328 | 2 | 1790 ± 040 | 1.91 | 0.35 ± 0.005 |
| B2111+46 | 1.0147 | 333 | 1 | 800 ± 190 | 1.66 | 0.28 ± 0.04 |
| | | 333 | 2 | 1230 ± 50 | 2.54 | 0.41 ± 0.01 |

^aCone numbering is the same as in GG2001 and GG2003 (ie. from the innermost cone outwards).

Note. — The values of θ'_{fp} have been calculated for $r_{\text{cr}} \ll h_{\text{em}}$. Had the assumption been not satisfied (as is probably the case at least for B0450–18), they should be understood as upper limits. Errors of θ'_{fp} are substantially underestimated, because they do not include uncertainty in α and β .

Table 2. The applicability of different methods of determining r to different kind of available data.

| Data needed | Analysis method |
|--|--------------------------|
| M or T profile only | this work (eq. 7), OERPS |
| profile of any type + position angle curve | geometric, BCW |

Note. — M and T respectively mean ‘multiple’ and ‘triple’ pulse profiles according to the classification scheme of Rankin (1983). OERPS stands for the ‘outer edge relativistic phase shift method’ (Section 3) and BCW for the delay-radius method of Blaskiewicz et al. (1991).

Table 3. Surface colatitudes θ'_{fp} of magnetic field lines associated with the 10% intensity level, derived with the method of BCW91.

| Pulsar | ν [GHz] | θ'_{fp} | $\pm 1\sigma$ error box | LOC ^a [σ] |
|----------|-------------|-----------------------|-------------------------|-------------------------------|
| B0301+19 | 0.43 | 1.97 | 1.38 – 2.64 | 1.7 |
| | 1.42 | 3.03 | 1.97 – 4.65 | 2.1 |
| B0525+21 | 0.43 | 2.28 | 1.70 – 3.16 | 2.6 |
| | 1.42 | 1.82 | 1.29 – 2.89 | 1.8 |
| B1913+16 | 0.43 | 1.13 | 0.77 – 1.44 | 0.4 |
| | 1.42 | 0.91 | 0.69 – 1.12 | 0.4 |
| B1914+13 | 1.42 | 0.71 | < 0.80 | 2.3 |

^alevel of consistency of θ'_{fp} with 1, in units of the standard deviation σ derived from errors of r_{delay} and r_{geo} from table 3 in Blaskiewicz et al. (1991).

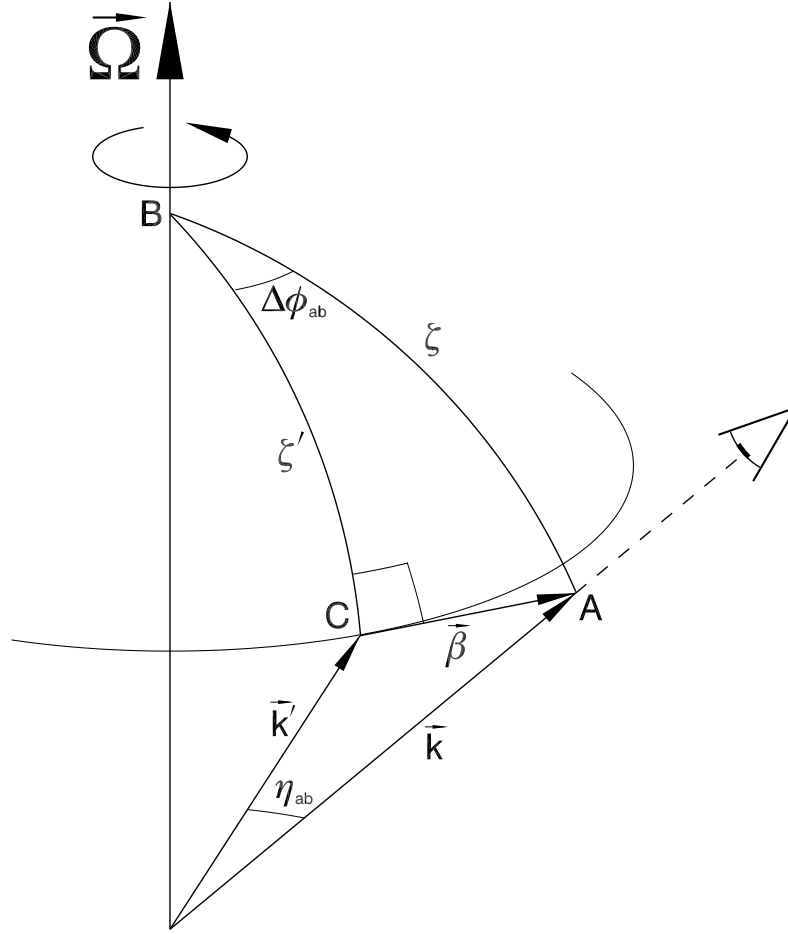


Fig. 1.— Illustration of the geometry considered in the derivation of eq. (5) (Appendix A).